

Regional administration of oncolytic Echovirus 1 as a novel therapy for the peritoneal dissemination of gastric cancer

Erin S. Haley · Gough G. Au · Brian R. Carlton ·
Richard D. Barry · Darren R. Shafren

Received: 10 September 2008 / Revised: 27 November 2008 / Accepted: 3 December 2008 / Published online: 13 January 2009
© Springer-Verlag 2008

Abstract The dissemination of malignant gastric cells to the peritoneum occurs frequently, usually as an early event in disease, and results in poor patient prognosis. Surgery and chemotherapy offer limited therapeutic success. The low-pathogenic human enterovirus, Echovirus 1 (EV1), is an oncolytic virus that selectively targets and destroys malignant prostate and ovarian cancer xenografts in vivo. Lytic EV1 infection requires the cell surface expression of $\alpha_2\beta_1$, an integrin involved in the dissemination of gastric cancer cells to the peritoneum. Herein, we evaluated the capacity of EV1 for anti-neoplastic cell action in gastric peritoneal carcinomatosis. Flow cytometric analysis demonstrated that $\alpha_2\beta_1$ was abundantly surface expressed on a panel of gastric cancer cell lines, rendering the majority of lines highly susceptible to in vitro lytic EV1 infection and supportive of efficient viral progeny production. A bioluminescent MKN-45-Luc SCID mouse model of peritoneal dissemination was developed to allow real-time non-invasive monitoring of peritoneal tumor burden. Employing this mouse model, we demonstrated a therapeutic dose-response for escalating oncolytic EV1 doses. Taken together, these results emphasize the exciting potential for

EV1 as a single or adjunct therapy for the control of the peritoneal dissemination of gastric cancer.

Keywords Echovirus 1 · Oncolytic virus · Virotherapy · Gastric cancer · Peritoneal dissemination

Introduction

Gastric cancer is the fourth most common type of cancer and the second most common cause of cancer-related mortalities worldwide. Almost two thirds of cases occur in the developing world [1]. In the United States and Europe, the 5-year survival rate is less than 20% as detection usually occurs in the late stage of disease [2]. Peritoneal carcinomatosis (PC) or dissemination in gastric cancer occurs frequently and early, with PC staging usually advanced at diagnosis of the primary cancer. The median survival for patients with PC is 3.1 months [3]. In the absence of early carcinomatosis in gastric cancer patients, the peritoneum is the most common site of recurrence following surgical resection of primary lesions [4]. Traditionally, the survival advantage offered by surgery or systemic chemotherapy for disseminated peritoneal disease is limited [5, 6]. Recent studies have demonstrated some success with cytoreductive surgery for the removal of macroscopic lesions, in combination with intraoperative peritoneal hyperthermic chemotherapy for the elimination of micrometastases and free cancer cells [7]. Regardless, the inherent toxicities associated with chemotherapy suggest that investigation of novel therapies for PC is warranted.

An innovative potential anti-neoplastic strategy for the treatment of PC is oncolytic virotherapy, which involves the use of either genetically engineered or naturally occurring

E. S. Haley · G. G. Au · R. D. Barry · D. R. Shafren (✉)
The Picornavirus Research Unit, School of Biomedical Sciences,
Faculty of Health, The University of Newcastle,
Newcastle, NSW 2300, Australia
e-mail: dshafren@mail.newcastle.edu.au

B. R. Carlton
Animal Services Unit, The University of Newcastle,
Newcastle, NSW 2300, Australia

D. R. Shafren
Viralytics Ltd,
Unit 8, 33 Ryde Road,
Pymble, NSW 2073, Australia

viruses, which specifically target and lyse malignant cells while leaving surrounding non-malignant cells relatively unharmed [8, 9]. Engineered oncolytic Herpes simplex viruses (HSVs) and adenoviruses are under preclinical assessment for the targeting and control of gastric PC [10–14]. Another group of oncolytic viruses, which exhibit anti-tumor efficacy in a range of malignancies, are the naturally occurring low-pathogenic human enteroviruses; Coxsackievirus A21 (CVA21), its associated decay accelerating factor (DAF)-using variant (CVA21-DAFv) and Echovirus 1 (EV1) [15–19]. In vitro and in vivo challenge studies have demonstrated that EV1, which interacts specifically with the I domain of the viral receptor integrin $\alpha_2\beta_1$ on the cell surface [20, 21], displays efficacy in an ovarian peritoneal ascites cancer model [19]. The binding of extracellular matrix (ECM) proteins, type I collagen and/or laminin by $\alpha_2\beta_1$ on the surface of malignant gastric cells is proposed to play a major role in cellular invasion and dissemination [22–24]. Immunohistochemical analysis of gastric tumor biopsy samples has revealed that the expression of $\alpha_2\beta_1$ on the surface of peritoneal disseminated cells is significantly greater than that of the associated primary gastric lesion [25]. Furthermore, a specific role for $\alpha_2\beta_1$ in the natural seeding of gastric cancer cells to the peritoneum in mouse models of PC is proposed [22, 24, 26], suggesting that the specific targeting of $\alpha_2\beta_1$ may be an effective treatment for PC. EV1 and type I collagen bind to different residues in the I domain of the α_2 subunit, however, the $\alpha_2\beta_1$ integrin cannot bind EV1 and type I collagen simultaneously. Notably, EV1 binds $\alpha_2\beta_1$ with a tenfold increase in affinity compared to collagen [27, 28]. A molecule derived from *Streptomyces* which binds to the α_2 subunit I domain and inhibits adhesion to collagen, is potentially therapeutic [29], however this molecule also binds to the I domain of other collagen binding subunits; α_1 , α_{10} , and α_{11} as a result of their structural similarity. The binding of EV1 to $\alpha_2\beta_1$, in contrast, is specific to this integrin complex.

EV1 was originally isolated from the stools of individuals in the absence of symptomatic infection [30], suggesting that the pathogenicity of the virus is low. Comparable to CVA21, which has proven to be tolerable when deliberately administered via the intra-nasal route to humans [31], EV1 infection is reported to be associated with some mild upper respiratory infections [32]. In vitro infectivity studies utilizing EV1 have demonstrated that non-malignant human prostate and ovarian cell lines are poorly permissive to infection and peripheral blood mononucleocytes (PBMCs) are refractile to infection [18, 19], indicative of a restricted tissue tropism for the virus. The exploitation of the elevated surface expression of $\alpha_2\beta_1$ as a biological target of EV1, on malignant cells compared to surrounding normal cells, highlights its potential role as a more suitable therapeutic candidate than standard chemotherapy regimes.

An additional valuable attribute possessed by EV1 and other replication-competent oncolytic viruses over traditional anti-cancer therapies, is that the initial challenge dose has the potential to be amplified within the cells of the targeted tumor. Following the infection of a malignant cell, infectious progeny virus is produced and expelled when the cell undergoes lytic rupture, thus enabling the potential infection of surrounding malignant cells. In this way, the virus is amplified while malignant cells are present and supportive of viral replication, enabling viral spread and destruction of metastatic cells at sites distant to the original point of administration [19].

In this light, we evaluated the therapeutic potential for EV1 as an oncolytic agent for the control of gastric PC. The expression of integrin $\alpha_2\beta_1$ on the surface of a panel of gastric cancer cell lines was assessed using flow cytometric analysis, and their capacity to support EV1 replication and subsequent lytic infection was assessed through the utilization of in vitro lytic infectivity techniques. Subsequently, a dose ranging efficacy study of oncolytic EV1 was evaluated in a bioluminescent model of peritoneal dissemination of human gastric cancer xenografts in immune-compromised mice. The results presented herein, highlight the exciting potential for EV1 as a single or adjunct therapy for peritoneal dissemination of gastric cancer.

Materials and methods

Cells and cell culture conditions

The gastric cancer cell lines; AGS, Hs746T, and NCI-N87 were obtained from the American Type Culture Collection (ATCC). The gastric cancer cell line MKN-45 was obtained from Dr. Sara Linden (Mater Medical Research Institute, South Brisbane, Australia). The ovarian cancer cell line DOV13 was obtained from the Peter MacCallum Cancer Centre (Melbourne, Australia). NCI-N87, MKN-45, and DOV13 cells were routinely propagated in RPMI supplemented with 10% FCS, L-glutamine, sodium pyruvate, Hepes, and antibiotics. The AGS cells were propagated in Kaighn's Modified F12 containing 10% FCS and antibiotics. The Hs746T cells were propagated in Dulbecco's Modified Eagle Medium supplemented with L-glutamine, sodium pyruvate, Hepes, antibiotics, and 10% FCS. All cell lines were propagated at 37°C in a 5% CO₂ atmosphere. Cell lines were routinely tested for the absence of Mycoplasma using the MycoSensor™ QPCR Assay Kit (Stratagene, Mount Waverley, Australia).

Viruses and virus purification

The prototype strain of EV1 (*Farouk*) virus stock was obtained from Dr. Margery Kennett (Entero-respiratory

Laboratory, Melbourne, Australia). Semi-purified stocks of EV1 were prepared for use in *in vitro* protocols as follows; EV1 was propagated in DOV13 cells, infected cells were then freeze-thawed and the supernatant obtained by clarification at 4°C, 1,000×g for 10 min. Semi-purified virus stocks were stored in single-use aliquots at –80°C. Purified virus stocks were prepared for use in animal procedures via propagation in DOV13 cells followed by purification by velocity centrifugation on 5–30% sucrose gradients. The peak infectious fractions were pooled, dialyzed against phosphate buffered saline (PBS) and stored as single-use aliquots at –80°C. Stocks were titrated by micro-plate tissue culture infectivity dose assays on DOV13 cells, to determine the fifty percent tissue culture infectivity dose per milliliter (TCID₅₀/mL) and titres calculated using the method by Karber [33].

Antibodies and vectors

The anti- α_2 (AK7) monoclonal antibody (mAb) recognizes the α_2 sub-unit of the $\alpha_2\beta_1$ integrin and was a gift from Dr. Michael Berndt (The Baker Institute, Melbourne, Australia). The anti-enterovirus (clone 5-D8/1) mAb (DAKO, Copenhagen, Denmark) was produced against heat-inactivated Coxsackievirus B5 (CVB5) and reacts with an epitope on the VP1 peptide which is highly conserved within the enterovirus group [34, 35].

The Ubiquitin-driven luciferase gene-encoding lentivirus vector was a gift from Dr. J. Shay (University of Texas Southwestern Medical Centre, Dallas, USA) and was constructed previously as described [36].

Generation of stable luciferase expressing gastric cancer cell transfectants

MKN-45 cells were propagated in a 6-well plate in RPMI containing 10% FCS until they reached 60% confluency. DEAE-Dextran was diluted in 10% RPMI (1:1,000) and 3 mL of the mixture added directly to the cell monolayer. One hundred microliters of the luciferase gene-expressing lentivirus vector was added to the media and the cells incubated at 37°C in a 5% CO₂ atmosphere for 24 h. Cells were divided into 12 wells of a 12-well plate and G418 (Promega, Sydney, Australia) (400 µg/mL) selection applied for 72 h. The G418 selection was then reduced (200 µg/mL) and maintained for 2 weeks to enable growth of stable transfectant clones. Each of the clones were tested for luciferase expression and the brightest clone, herein referred to as MKN-45-Luc, further characterized. Briefly, cells were diluted to cover a range from 100,000 to ten cells in RPMI in a black 96-well plate. A media-only well was included as a control. To lyse the cells, 25 µL of 1× lysis buffer (Promega) per well was added, prior to the addition of

50 µL of luciferase substrate reagent (Promega). The bioluminescence was examined immediately by scanning for 30 s at a high resolution using the IVIS™ Imaging System (Xenogen, CA, USA), comprised of a highly sensitive, cooled charge coupled (CCD) camera mounted in a light-tight specimen chamber, which detected and digitized the light being emitted by the cells, and electronically displayed a pseudocolor image. Living Image® software (Xenogen) was used to draw a region of interest around the wells and the bioluminescence quantified as average radiance (photons/s/cm²/r).

Flow cytometry

Flow cytometric analysis was utilized to analyze the level of surface expression of the EV1 receptor, integrin $\alpha_2\beta_1$, on the surface of gastric cancer cell lines. Sub-confluent monolayers of cells were dispersed by treatment with versene. Dispersed cells (1×10^6) were then pelleted by centrifugation at 1,000×g for 5 min at 4°C, resuspended in 100 µL of the α_2 (AK7) monoclonal antibody (5 µg/mL) in PBS and incubated on ice for 20 min. Cells were then washed with PBS and pelleted as above. Cells were then resuspended in 100 µL of R-phycoerythrin-conjugated (RPE) F(ab')₂ fragment of goat anti-mouse immunoglobulin diluted 1:100 in PBS (DAKO) and incubated on ice for 20 min. Cells were then washed, pelleted, resuspended in PBS, and analyzed for receptor expression using a FACScanto™ flow cytometer (Becton Dickinson, Sydney, Australia), with data analyzed using Weasel v2.1 software (WEHI Biotechnology Centre, Melbourne, Australia) and results expressed as histograms.

In vitro EV1 infectivity assay and mAb blocking assay

To determine the susceptibility of gastric cancer cell lines to *in vitro* lytic EV1 infection, gastric cancer cells were seeded in 96-well plates and propagated to 50–80% confluency in the appropriate medium (described above) containing 2% FCS. Cell monolayers were challenged with tenfold serial dilutions of semi-purified virus (titre 3.2×10^7 TCID₅₀/mL), standardized on DOV13 cells, (100 µL in quadruplicate) in medium containing 2% FCS and incubated at 37°C in a 5% CO₂ environment for 72 h. Cell monolayers that exhibited cytopathic effect (CPE) upon microscopic examination were scored as positive and TCID₅₀ calculated. Utilizing these infectious titres, the multiplicity of infection (MOI) of EV1 required to induce detectable CPE in each cell line was calculated. The results are presented as the mean (±SEM, standard error of the mean) of three independent experiments. An MOI of ≤ 1 TCID₅₀/cell was arbitrarily designated as a challenge dose, which determines whether a cell line is susceptible to oncolytic enteroviral infection.

Photomicrographs of gastric cancer cells infected with EV1 (MOI=1) were taken at 72 h post-infection using an Olympus IX70 inverted microscope ($\times 100$ original magnification) and DP70 digital camera (Olympus, Mount Waverley, Australia).

To measure EV1-mediated cytotoxicity, gastric cancer cells were propagated in 96-well plates and infected with tenfold serial dilutions of EV1 (100 μL in quadruplicate) (starting MOI=10), and the quantity of lactate dehydrogenase (LDH), an enzyme released upon cell lysis, in the culture supernatant measured at 24 h post-infection, using the CytoTox 96[®] Non-Radioactive Cytotoxicity Assay (Promega). Specifically, LDH was quantitated based on the conversion of a tetrazolium salt into a red formazan product. Absorbance was measured at 492 nm using a FLUOStar OPTIMA microplate reader (BMG LAB-TECH, Mornington, Australia). Cytotoxicity results are expressed as the mean (\pm SEM) percentage of the LDH yield in the highest viral dilution if 100% lysis was evident, or as a percentage of the LDH released in a 100% cell lysis control, which ever was greater for the individual cell line.

To demonstrate the specificity of EV1 for the $\alpha_2\beta_1$ receptor, MKN-45 gastric cancer cell monolayers in a 96-well plate were pre-treated with AK7 mAb (20 $\mu\text{g}/\text{mL}$) or RPMI containing 2% FCS (50 μL) as a control for 1 h at 37°C. Cell monolayers were then challenged with tenfold serial dilutions of EV1 (100 μL in triplicate) (starting MOI=8) in RPMI containing 2% FCS and incubated at 37°C in a 5% CO₂ environment for 72 h. Cell survival was assessed via microscopic examination, followed by incubation with crystal violet/methanol solution (0.1% crystal violet, 20% methanol, 20% formaldehyde in PBS) (100 $\mu\text{L}/\text{well}$) for 24 h, followed by three washes in distilled water.

Characterization of viral growth in gastric cancer cell monolayers

To investigate the replication kinetics of EV1 in gastric cancer cell lines, cells were plated in 24-well plates in medium containing 2% FCS and propagated for approximately 18 h to reach 80% confluency. Cells were infected with EV1 (MOI=10) and allowed to adsorb for 1 h at 37°C. Cells were washed three times with media to remove unbound virus and fresh 2% media added to the cells. Cells were incubated at 37°C in a 5% CO₂ environment and harvested at various time points up to 72 h post-infection. To harvest, cells and associated supernatants were freeze-thawed three times and the lysates centrifuged at 20,800 \times g for 2 min at 4°C. To assess total virus yield at each time point, the supernatants were titrated on 96-well plates of DOV13 cells, according to the 50% end-point tissue culture infectivity procedure described above.

SCID mouse model of peritoneal dissemination of gastric cancer and virus therapy

All animal work was performed according to guidelines approved by the University of Newcastle Animal Care and Ethics Committee (ACEC approval number 1089 0209). Severe Combined Immunodeficient (SCID)-Balb/c mice, of 6–8 weeks of age, were obtained from the Australian Research Council (ARC) (Perth, Australia) and were housed under specific-pathogen-free (SPF) conditions within the university animal holding facility. Mice were allowed to acclimatize to their environment for 1 week prior to the commencement of the experimental protocol.

MKN-45-Luc cells were grown in media containing 10% FCS, harvested and washed twice in PBS. Cell viability was assessed via trypan blue staining as cellular viability greater than 95% was required for xenotransplantation. Cells were resuspended in sterile PBS and kept on ice to maintain viability. Prior to cell injection, mice were anesthetized via isoflurane inhalation (4 L/min, maintained at 2%). Thirty-two female 6–8-week-old SCID-Balb/c mice were given intra-peritoneal injections of 5×10^6 MKN-45-Luc cells in a final volume of 500 μL . A group of eight mice did not receive tumor cells in order to serve as no tumor weight controls (NTC). Five days after cell injection, groups of eight mice were treated with intra-peritoneal sterile PBS, or one of 1×10^3 TCID₅₀, 1×10^5 TCID₅₀, or 1×10^7 TCID₅₀ EV1. Mice were visually monitored daily and weighed every 3 to 4 days. In vivo bioluminescent imaging was performed on the day of treatment and weekly, thereafter, using an IVIS[™] Imaging System (Xenogen). Briefly, mice were given an intra-peritoneal injection of *d*-Luciferin (Xenogen) (5 mg/mL in PBS) and anesthetized via isoflurane inhalation (4 L/min, maintained at 2%) prior to imaging at high resolution for 5 s. Bioluminescent images and measurements were acquired and analyzed using Living Image[®] software (Xenogen). Bioluminescent images were presented as bioluminescence overlaid on photographic images. Mice were euthanized if a weight loss of $\geq 20\%$ from the day of cell injection occurred. Serum samples were taken via the saphenous vein 1 h post-treatment and once weekly, thereafter, and stored at -80°C , prior to processing. Serum was analyzed for the presence of infectious EV1 according to the endpoint titration infectivity assay described above (100 μL in triplicate on DOV13 cells). Mice were monitored over a 42-day period. Upon sacrifice/euthanasia, laparotomies were performed. Tumor nodules were counted and the major stomach-associated nodule photographed, fixed in 10% neutral buffered formalin and paraffin embedded. NTC mice were not subject to anesthesia, bioluminescent imaging or saphenous vein bleeding during this protocol.

Histology

Hematoxylin and Eosin (H&E) staining was carried out to visualize tissue organization. Briefly, paraffin-embedded tumor sections were deparaffinized with xylene and rehydrated through a graded ethanol series. Nuclei were stained in Carazzis Hematoxylin (Fronine Laboratory Supplies, Riverstone, Australia), differentiated in acid alcohol (70% EtOH and 0.5% HCl) and blued in Scott's Tap Water Substitute Solution (Sigma-Aldrich, Castle Hill, Australia). Connective tissue was stained with Eosin (Sigma-Aldrich). Stained tissue sections were dehydrated and mounted in DPX (ProSciTech, Kirwan, Australia). Stained sections were viewed using a BX41 System microscope (Olympus) and photomicrographs taken ($\times 100$ original magnification) using a ColorView I Soft Imaging System CCD camera (Olympus).

Immunohistochemistry (IHC) was utilized for the visualization of EV1 capsid protein in tumor tissue. Sections were deparaffinized and rehydrated, as described above. Heat-induced antigen retrieval was carried out in Citrate Buffer (pH 6.0). IHC was carried out using the Vectastain Peroxidase Mouse IgG ABC Kit (Vector Laboratories, Brisbane, Australia) according to the manufacturer's protocol. Briefly, tissue endogenous peroxidase was blocked in 0.3% H_2O_2 in methanol for 30 min at room temperature. Tissue sections were then washed in PBS and blocked for non-specific staining with diluted horse serum (Vectastain ABC Kit) for 20 min at room temperature before being incubated with the primary anti-enterovirus mAb (clone 5-D8/1) (1:250) or pooled murine IgG (Biocare Medical, CA, USA) as a negative control, at 4°C overnight. Tissue sections were then washed and incubated with the VECTASTAIN biotinylated secondary antibody for 30 min at room temperature. Following washing, the tissues were incubated in VECTASTAIN ABC reagent for 30 min at room temperature followed by the addition of Diaminobenzidine (DAB) (Sigma-Aldrich), resulting in dark staining of the EV1 antigen. Tissues were then counterstained with Mayer's Hematoxylin (DAKO) and Scott's Tapwater Substitute Solution to stain the cell nuclei. Stained tissue sections were dehydrated and mounted in DPX. Photomicrographs ($\times 100$ and $\times 200$ original magnification) were taken as described above.

Statistics

Linear regression analysis was performed to correlate MKN-45-Luc cell number with bioluminescence. One-way ANOVA followed by the Bonferonni test for multiple comparisons was used to compare differences in percentage weight change and difference in percentage change in bioluminescence (total flux) from the day of treatment,

between treatment groups. One-way ANOVA followed by the Bonferonni test for multiple comparisons was also used to compare differences in serum viremia levels. Kaplan–Meier plots were used to represent survival of mice post-treatment and survival compared using the log-rank (Mantel-Cox) test followed by the Bonferonni test for multiple comparisons.

Results

Lytic EV1 infection of gastric cancer cells in vitro

Flow cytometric analysis was utilized to investigate the in vitro surface expression of $\alpha_2\beta_1$, required for EV1 infection, on a panel of gastric cancer cell lines. Cell surface receptor expression, presented as histograms, show that abundant levels of $\alpha_2\beta_1$ were displayed by all gastric cancer cell lines (Fig. 1a). An antibody blockade study was employed to confirm that the expression of $\alpha_2\beta_1$ on the surface of gastric cancer cells was required for EV1 cell binding, entry, and lytic infection. The lack of detectable cytopathic changes in cell morphology of the MKN-45 cell monolayer when pre-treated with anti- α_2 mAb and challenged with varying input multiplicities of EV1 (Fig. 1b), in comparison to EV1 infected cells in the absence of the mAb, was indicative of this $\alpha_2\beta_1$ receptor-mediated route of EV1 infection.

Having demonstrated the presence of high levels of $\alpha_2\beta_1$ integrin on the surface of gastric cancer cells, we next quantitatively investigated the degree of susceptibility of the cell lines to EV1-mediated oncolysis. LDH release was measured to correlate EV1-mediated cytotoxicity with viral input multiplicity in infected gastric cancer cell monolayers (24 h post-infection) (Fig. 2a). Each of the cell lines, except Hs746T, displayed 100% cytotoxicity at an input multiplicity of 10 TCID₅₀/cell. The AGS and MKN-45 cells displayed similar profiles with a reduction in cytotoxicity correlating with decreasing levels of viral challenge. However, the NCI-N87 cells were comparatively less susceptible to EV1-mediated cytotoxicity with lower EV1 input multiplicities. Lytic cell infectivity assays were undertaken and an endpoint titre calculated to determine the minimum input multiplicity of EV1 required to result in detectable cellular oncolysis, as evidenced by the development of CPE (72 h post-infection). The mean minimum input multiplicity (\pm SEM) required in each cell line from three independent experiments is presented (Fig. 2b). An $MOI \leq 1$ was arbitrarily designated to indicate that a cell line is considered susceptible to EV1-mediated oncolysis. EV1 demonstrated widespread, potent oncolytic activity in cells displaying variable morphologies, with complete CPE in three of the four cell lines evident following EV1 infection

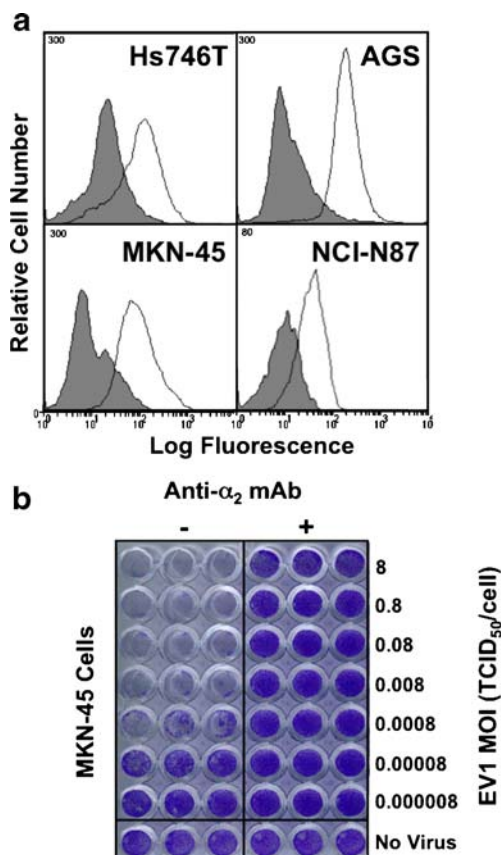


Fig. 1 Expression levels of $\alpha_2\beta_1$ on the surface of gastric cancer cells. **a** Cell lines were incubated with anti- α_2 monoclonal antibody (AK7) or RPE-conjugate alone and analyzed via flow cytometry. The filled grey histograms represent the binding of the conjugate and the black line histograms represent $\alpha_2\beta_1$ expression. **b** MKN-45 cell monolayers were pre-incubated with anti- α_2 monoclonal antibody (AK7) (20 $\mu\text{g}/\text{mL}$) prior to infection of cells with tenfold serial dilutions of EV1 (starting MOI=8). Following incubation at 37°C for 72 h, monolayers were fixed and stained with crystal violet solution to assess cell viability

at an input multiplicity of 1 (Fig. 2c). Monolayers of MKN-45 cells were the most susceptible to lytic EV1 infection over the 72 h time-period, requiring a mean of 3.3×10^{-6} TCID₅₀/cell for the induction of visible CPE, while AGS cells required 1.3×10^{-5} TCID₅₀/cell and NCI-N87 cells required 0.03 TCID₅₀/cell. Hs746T cells, however, required a mean input multiplicity of greater than 1 TCID₅₀/cell.

An important attribute of oncolytic virus therapy is that following lytic viral infection of malignant cells, viral replication results in a substantial amplification of the input viral load. One-step growth kinetics assays were undertaken to investigate whether EV1 resulted in viral amplification following infection of a panel of gastric cancer cell lines

(Fig. 3). Infection of the three susceptible lines (requiring an MOI \leq 1); AGS, NCI-N87, and MKN-45, resulted in an approximate 100-fold increase in viral yield in the 12 h post-infection. Following this, there was an apparent decrease in virus yield due to complete lysis of the cell monolayer at this point. In contrast, the Hs746T cell line, which required a higher input multiplicity of EV1 for lytic infection (Fig. 2b), produced infectious progeny until 24 h post-infection, though at a slower rate than those observed in the more susceptible lines. Incomplete CPE was evident in the infected Hs746T cells 72 h post-infection (data not shown) indicating that a subset of cells may have been refractile to infection or in a steady state of persistent infection.

Oncolytic EV1 therapy in an in vivo model of peritoneal dissemination of gastric cancer

Having demonstrated that EV1 was efficacious as an oncolytic agent in in vitro cultured gastric cancer cells, we next determined whether oncolytic EV1 treatment could be effectively utilized to target and destroy malignant cells in an in vivo murine model of peritoneal dissemination of gastric carcinoma. The well-characterized gastric cancer cell line, MKN-45 naturally seeds to the peritoneum of SCID mice through its expression of $\alpha_2\beta_1$ [26]. To enable non-invasive in vivo bioluminescent imaging of tumor burden, MKN-45 cells were stably transfected with the firefly luciferase gene, generating the MKN-45-Luc cell line. To assess the sensitivity of the luciferase expressing line, MKN-45-Luc to bioluminescent detection, cells were diluted in a 96-well black plate and submitted to bioluminescent imaging (Fig. 4a). The minimum number of detectable cells in suspension was 250 and the total cell number per well correlated well with bioluminescence ($R^2=0.99$) over a broad dynamic range (Fig. 4b). MKN-45-Luc cells and non-transfected MKN-45 cells displayed similar levels of surface $\alpha_2\beta_1$ expression and susceptibility to in vitro lytic EV1 infection (data not shown).

The bioluminescent MKN-45-Luc cells were injected via the intra-peritoneal route into SCID mice and xenografts allowed to form for 5 days. Mice were subsequently administered a low (1×10^3 TCID₅₀), medium (1×10^5 TCID₅₀) or high (1×10^7 TCID₅₀) intra-peritoneal dose of EV1. Non-invasive bioluminescent imaging, based on efficient luciferase expression by only viable tumor cells, was used to monitor and quantitate MKN-45-Luc tumor burden in mice on the day of virus administration and weekly, thereafter. The results are presented as percentage change in total flux (photons/s) (mean \pm SEM) from the day of treatment (Fig. 4c). Seven days post-treatment, there was a mean 28.75% increase in total flux in the PBS treated mice. This was significantly different ($p<0.05$) when

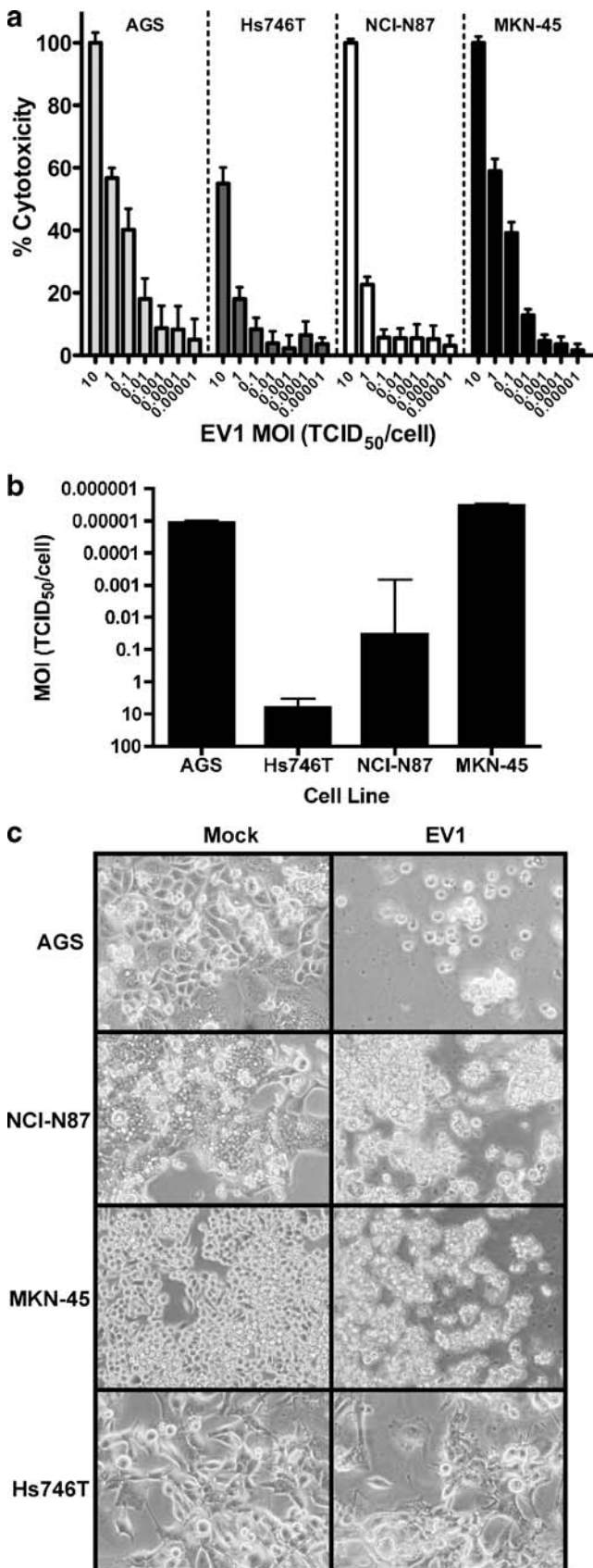


Fig. 2 Echovirus 1 oncolysis of gastric cancer cells in vitro. **a** Gastric cancer cell lines were propagated in monolayers in 96-well plates and infected with tenfold serial dilutions of EV1 (starting MOI=10). Following incubation at 37°C for 24 h, the level of LDH in the cell supernatant was quantitated as a measure of cytotoxicity. The data is presented as the mean percentage cytotoxicity (+SEM) compared to the 100% cytotoxicity observed at MOI=10 (AGS, MKN-45, NCI-N87) or in a 100% cell lysis control (Hs746T). **b** Gastric cancer cell lines were propagated as above and infected with tenfold serial dilutions of EV1 (3.2×10^7 TCID₅₀/mL). Following incubation at 37°C for 72 h, cell monolayers were examined microscopically for the presence of CPE. Fifty percent end-point titres were calculated using the method of Karber and the mean (+SEM) minimum MOI (TCID₅₀/cell) required to induce CPE for each cell line from three independent experiments was calculated. **c** Gastric cancer cell monolayers were infected with EV1 (MOI=1) and compared to mock infected monolayers. Photomicrographs were taken at 72 h post-infection ($\times 100$ original magnification)

compared to the 1×10^3 TCID₅₀ EV1 treated group (mean 47.38% decrease in total flux) and to the 1×10^5 and 1×10^7 TCID₅₀ treated groups (mean 68.5% and 71.5% decrease in total flux, respectively) ($p < 0.01$). This reduction in bioluminescence indicated that EV1 treatment resulted in a reduction in peritoneal tumor cell viability, however there was no significant difference in percentage change in total flux between each of the virus treatment groups. Following euthanasia of PBS-treated mice due to weight loss ($\geq 20\%$ from day of MKN-45-Luc cell injection), only three PBS-treated mice were alive on day 14 and two mice remained from days 21 to 35. All of the PBS-treated mice had been euthanized by 35 days post-treatment. Three of the eight 1×10^3 TCID₅₀ EV1-treated mice demonstrated an increased percentage change in total flux between days 14 and 28. However, 35 days post-treatment, the percentage change in total flux in the PBS treated group ($1.4 \times 10^4\%$ increase) was again significantly higher ($p < 0.01$) than that observed in each of the EV1

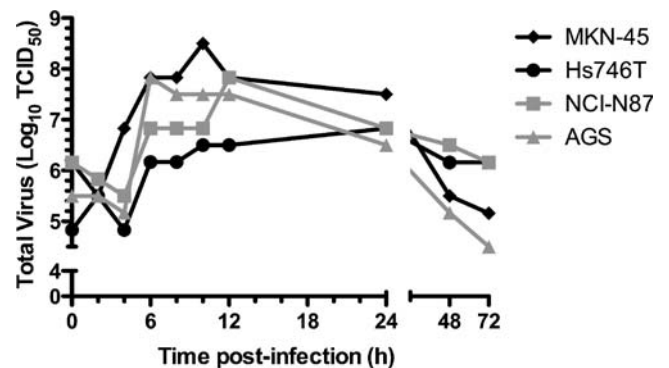


Fig. 3 Growth kinetics of EV1 in gastric cancer cells in vitro. The analysis of one-step growth kinetics was undertaken by infecting gastric cancer cell monolayers with EV1 (MOI=10). Cells and supernatants were then harvested at multiple time points (up to 72 h) post-infection, freeze-thawed three times and homogenates titrated on DOV13 cells. Fifty percent end-point titres were calculated for each cell line at each time point post-infection

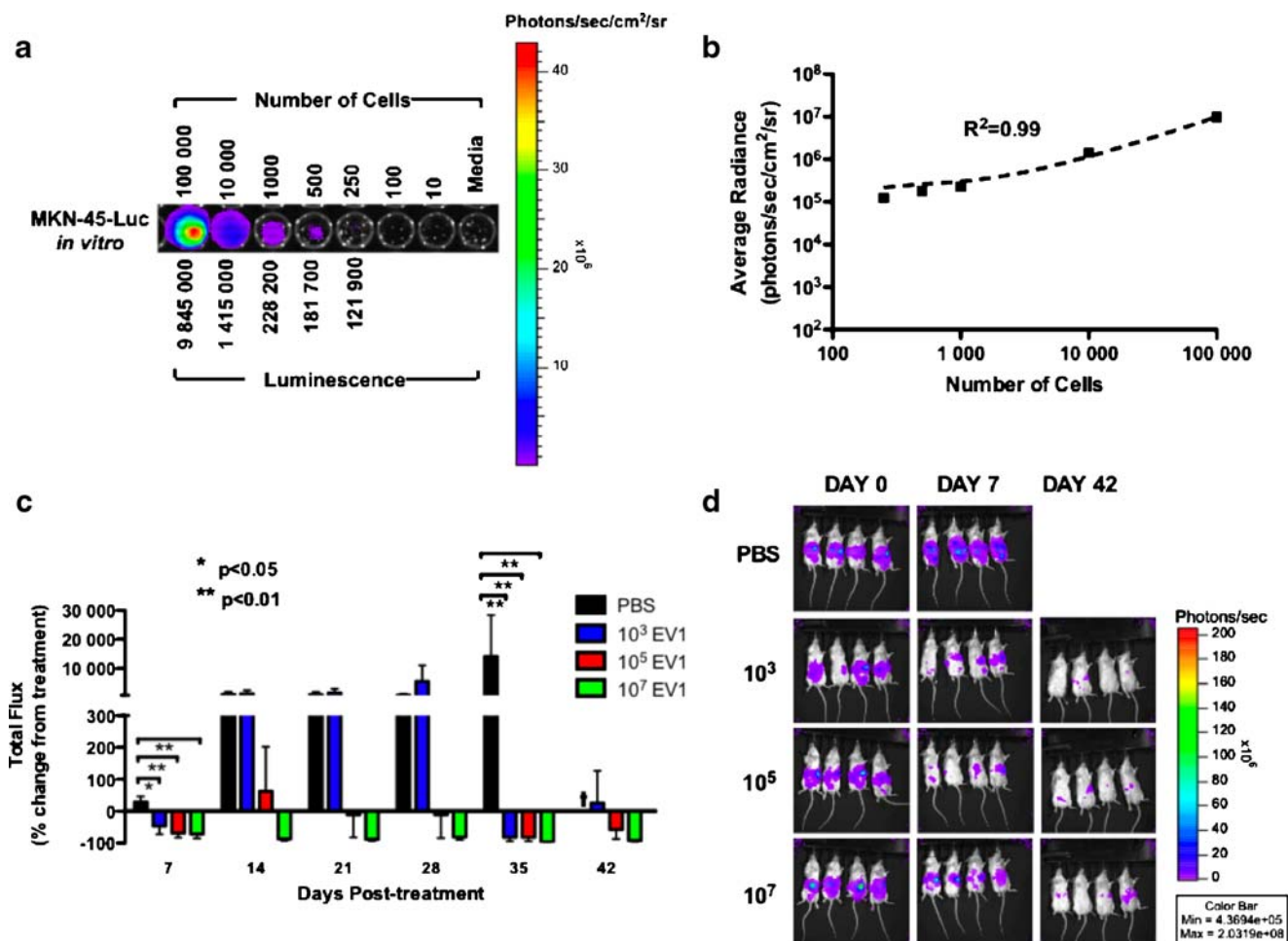


Fig. 4 Bioluminescence imaging of MKN-45-Luc tumor burden in a SCID mouse model of peritoneal dissemination, following intra-peritoneal EV1 administration. **a** MKN-45-Luc cells were diluted from 100,000 to ten cells in a 96-well black plate and imaged for bioluminescence at high resolution for 30 s following cell lysis and the addition of luciferase substrate, *d*-Luciferin. A media-only well served as a cell negative control. **b** Linear regression analysis was used for the determination of correlation between cell number per well and bioluminescence (average radiance=photons/s/cm²/sr) ($R^2=0.99$). **c** Female 6–8-week-old SCID-Balb/c mice were administered intra-peritoneal injections of 5×10^6 MKN-45-Luc cells ($n=32$). An additional group of mice received no tumor cells in order to serve as

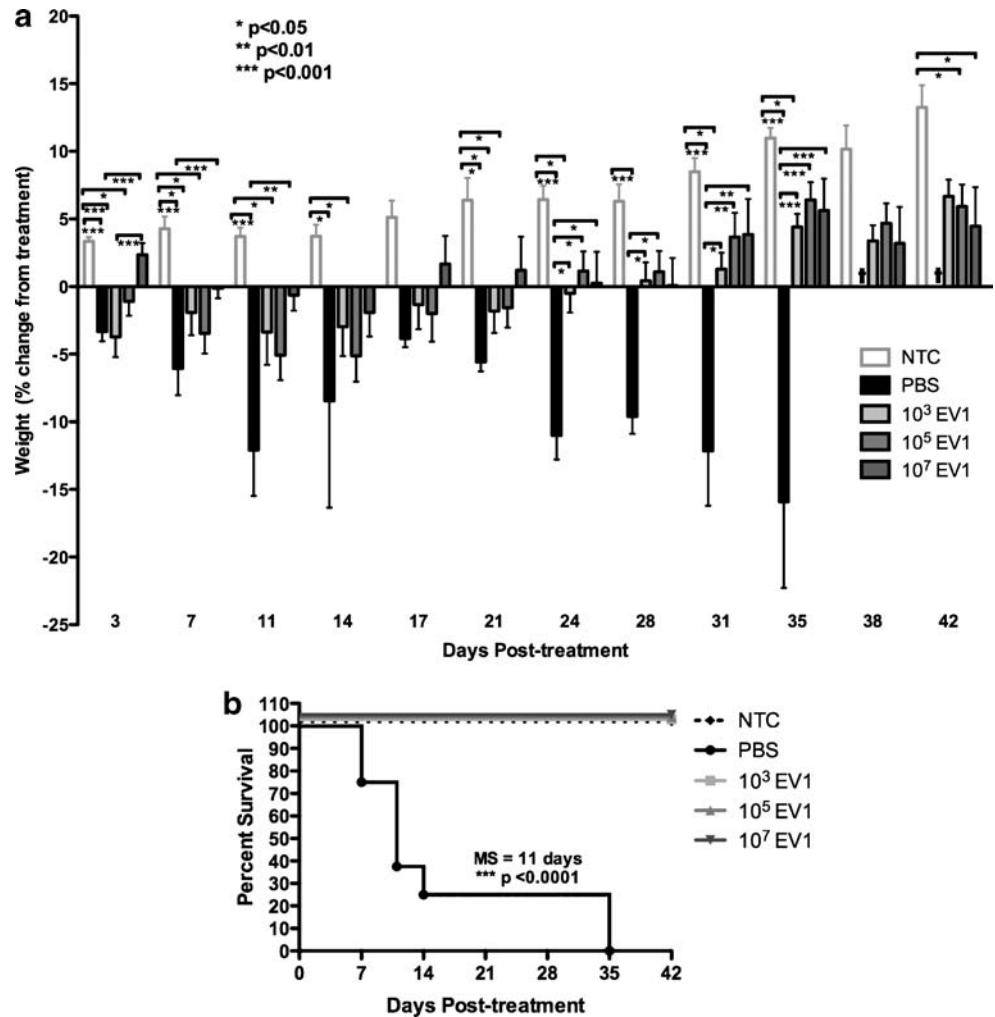
weight controls (NTC) ($n=8$). Five days after cell injection, mice were injected with sterile PBS, or one of; 1×10^3 , 1×10^5 , or 1×10^7 TCID₅₀ EV1 in sterile PBS ($n=8$ /group), via the intra-peritoneal route. Bioluminescence imaging was performed for 5 s using a high resolution setting following an intra-peritoneal injection of *d*-Luciferin, on the day of treatment and weekly, thereafter. Bioluminescence was computed as total flux (photon/s) and the mean percentage change (\pm SEM) from the day of treatment presented graphically. *Dagger* Indicates all PBS-treated mice had been euthanized prior to day 42. **d** Bioluminescent images representative of mice from each treatment group were compared for days 0, 7, and 42 days post-treatment

treatment groups (82.7%, 82.22%, and 96.63% decrease in the 1×10^3 , 1×10^5 , and 1×10^7 TCID₅₀ groups, respectively). At this time, there were no significant differences between the three EV1 treatment groups. Representative images of bioluminescence for each group are shown for days 0, 7, and 42 days post-treatment (Fig. 4d).

To evaluate the effects of peritoneal tumor burden on animal health, the mice were weighed on the day of treatment and every 3 to 4 days, thereafter, with data presented as percentage change in weight (mean \pm SEM) from the day of virus administration (Fig. 5a). The no tumor weight control (NTC) mice continually gained weight throughout the duration of the study and served as

a control for normal murine weight changes. The PBS-treated tumor-bearing mice lost weight steadily until 11 days post-treatment. However, an increase in mean percentage weight change of these mice between days 11 and 17 was observed due to the euthanasia of six of the eight mice (due to a loss of weight of $\geq 20\%$ from the day of cell injection) during the 7 to 14-day period. From day 17 post-PBS administration, the two remaining mice from this group suffered substantial weight loss and were euthanized 35 days post-treatment. The group of mice administered 1×10^3 TCID₅₀ EV1 initially lost body weight and then began gaining weight steadily from day 14 post-virus injection onwards. The percent change in body weight of

Fig. 5 Weight and survival of mice bearing peritoneal MKN-45-Luc xenografts following intra-peritoneal EV1 administration. **a** Mice were weighed on the day of treatment and every 3 to 4 days throughout the duration of the experiment. The percentage weight change from the day of treatment for each mouse was calculated. Mean percentage weight change (\pm SEM) from treatment over time is presented graphically. *Dagger* Indicates all PBS-treated mice had been euthanized by day 35. **b** Mice were euthanized when the percentage weight loss from the day of MKN-45-Luc cell injection was $\geq 20\%$. A Kaplan–Meier survival plot demonstrates that all PBS-treated mice had been euthanized by day 35 post-treatment. All other groups remained alive until day 42 when the experiment was terminated. *MS* median survival time



this group was significantly different from the PBS-treated group from day 24 onwards ($p < 0.05$) ($p < 0.001$ day 35). Furthermore, there was no significant difference between the percentage weight change from day of virus injection in this group, and the NTC group on days 35 and 42, upon termination of the experiment. The mice injected with 1×10^5 TCID₅₀ EV1 displayed weight loss at a slow rate until day 14, when they steadily began gaining weight, with a significant difference in percentage weight change between this group and the PBS-treated group observed from day 24 onwards ($p < 0.05$) ($p < 0.01$ day 31) ($p < 0.001$ day 35). No significant difference in percentage weight change was evident between this group and the NTC group, during days 24 and 38. The mice from the group that received 1×10^7 TCID₅₀ EV1 initially gained weight, followed by a slow rate of weight loss prior to an increase from day 14 post-virus injection onwards. A significant difference in percentage weight change between this group and the PBS-treated group was noted on days 3 and 7 ($p < 0.001$), day 11 ($p < 0.01$), day 24 ($p < 0.05$), and from day 31 onwards ($p < 0.01$, $p < 0.001$ day 35). At no time throughout the course of the experiment, except day 42, was there a significant

difference in percentage weight change between this group and the NTC group. Three days post-treatment, there was a significant difference ($p < 0.001$) between the 1×10^3 and 1×10^7 TCID₅₀ EV1-treated groups, indicating an initial dose-dependent effect. At no time-point throughout the experiment was there any significant difference in percentage weight change between the 1×10^3 and 1×10^5 TCID₅₀ EV1-treated groups or between the 1×10^5 and 1×10^7 TCID₅₀ EV1-treated groups. Importantly, it was not until day 28 that all of the EV1-treated groups displayed a positive percentage weight change from the day of treatment, an event that occurred on day 3, and again from day 17 onwards in the group treated with the highest EV1 dose (1×10^7 TCID₅₀), from day 24 by the mice treated with the medium dose (1×10^5 TCID₅₀) and finally, from day 28 in the group treated with the low dose of virus (1×10^3 TCID₅₀).

Kaplan–Meier survival analysis (Fig. 5b) demonstrated that the median survival time for the PBS-treated mice was 11 days post-treatment, with all mice euthanized by 35 days post-treatment (41 days post-cell injection). In comparison, 100% of mice that received each of the doses of EV1 were

alive when the experiment was terminated 42 days post-treatment (47 days post-cell injection). A statistically significant difference ($p < 0.0001$) in survival time existed between the PBS-treated mice and each of the treatment groups and NTC mice. No differences in survival rates were observed between those mice receiving any of the three doses of EV1. Importantly, no difference between the survival of the virus-treated mice and the NTC mice that had not received MKN-45-Luc cells at all, was observed. In addition, no signs of animal morbidity, which may be attributed to viral administration, were observed for the duration of the experiment.

The levels of circulating infectious EV1 in the blood were determined 1 h post-treatment and weekly thereafter, via end-point lytic titration on DOV13 cells (Fig. 6a).

On the day of virus administration, a significantly higher level of EV1 was detected in the circulation of the 1×10^7 TCID₅₀ group (mean = 1.3×10^6 TCID₅₀/mL) ($p < 0.01$) compared to that detected in the 1×10^3 and 1×10^5 TCID₅₀ treatment groups (mean = 1.5×10^3 and 6.9×10^3 TCID₅₀/mL, respectively). The calculated mean level of infectious virus in the 1×10^3 TCID₅₀-treated group on day 0 was subject to limitations imposed by the sensitivity of the assay and may have actually been lower. Viral loads detected in the circulation of each treatment group had equalized by 7 days post-treatment (mean = 4.3×10^7 TCID₅₀/mL). Twenty-eight days post-treatment, levels of circulating virus had decreased for each treatment group (mean = 3.7×10^5 TCID₅₀/mL) and remained steady until the experiment was terminated.

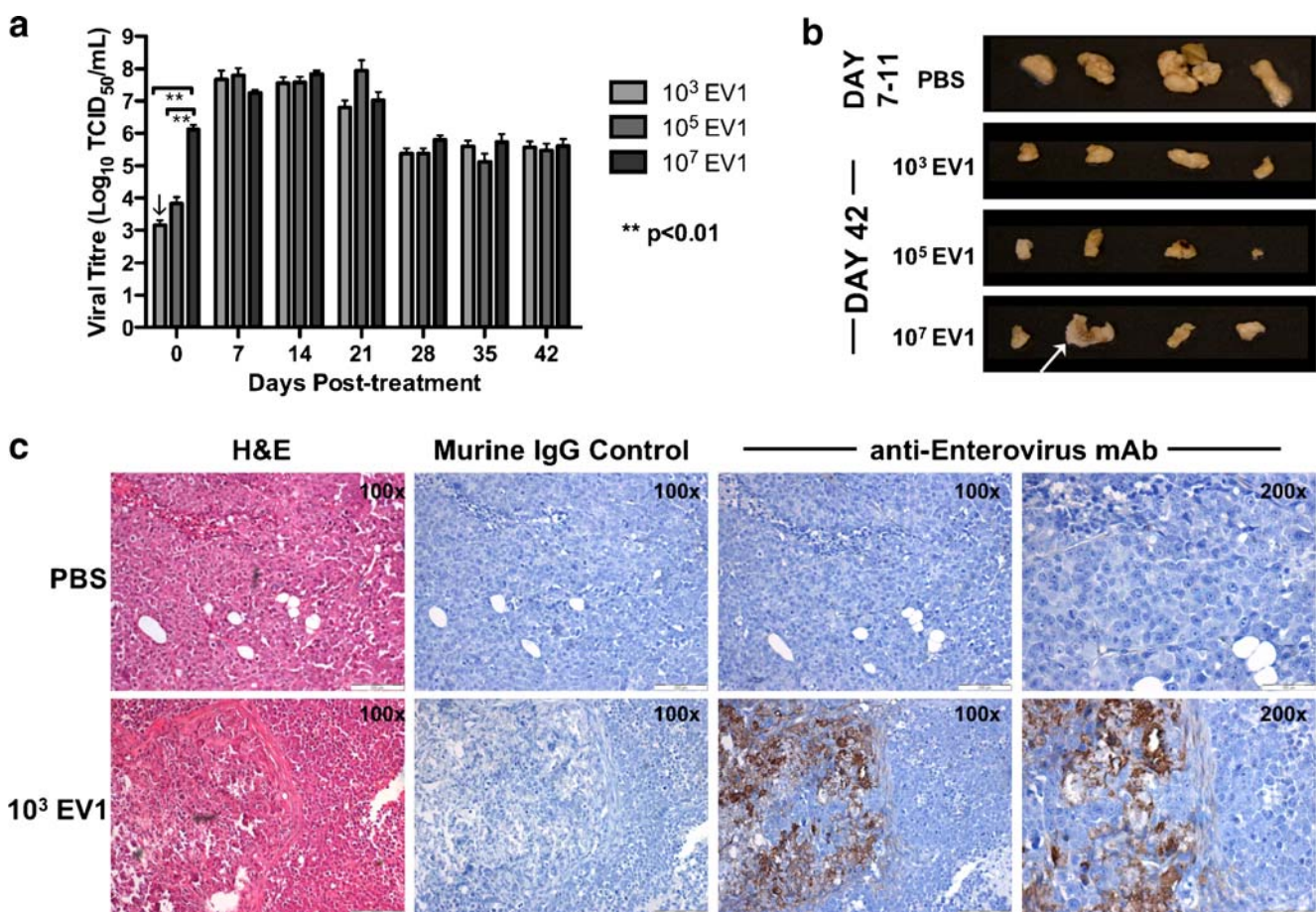


Fig. 6 Detection of EV1 in the serum and remaining MKN-45-Luc tumor nodules following intra-peritoneal virus administration. **a** Mice were bled via the saphenous vein 1 h post-treatment and weekly thereafter. Serum was assessed for the presence of infectious EV1 via end-point lytic titration on DOV13 cells. The mean viremia levels (TCID₅₀/mL) (\pm SEM) over time are presented graphically. The black arrowhead indicates a mean titre of 1.5×10^3 TCID₅₀ lay at the limit of sensitivity of the assay, due to constraints imposed by the volumes of serum attainable. It is possible that this result could be lower than that displayed. **b** The major stomach-associated tumor was excised and

photographed upon euthanasia of PBS mice (days 7 and 11) and upon sacrifice of EV1 treated mice (day 42). Representative tumors from each treatment group are shown. The white arrowhead indicates a fat deposit associated with the excised tumor. **c** The excised tumors were fixed and paraffin embedded. Tissue sections were H&E stained for the visualization of tissue structure and immunohistochemical analysis undertaken using the anti-enterovirus mAb (clone 5-D8/1) for the detection of EV1 protein in the tissue (dark staining). Photomicrographs of representative PBS-treated and 1×10^3 TCID₅₀ EV1-treated tumors are shown ($\times 100$ and $\times 200$ original magnification)

Upon euthanasia of PBS-treated mice, an exploratory laparotomy was performed to assess the anatomical distribution of the MKN-45-Luc tumor nodules. In seven of the eight mice, a large tumor was found associated with the greater curvature of the stomach via the greater omentum. Multiple smaller nodules were disseminated throughout the peritoneal cavity. In particular, these were located over the mesojejunum and along the mesenteric side of the jejunum. Very small nodules were also associated with the cardia of the stomach in conjunction with the abdominal portion of the esophagus. Upon sacrifice at day 42, laparotomies were performed on the virus-treated mice. The size of the major stomach-associated tumors in the virus-treated mice was noticeably smaller than those observed in the PBS-treated mice (Fig. 6b). Small nodules associated with the jejunum were located in two of the eight 1×10^3 TCID₅₀ and four of the eight 1×10^5 TCID₅₀ EV1-treated mice. Some small, disseminated nodules were also present in these groups. A similar result was found for the 1×10^7 TCID₅₀ EV1-treated mice. However, one of these mice had a large stomach-associated tumor, a dilated and fluid-filled intestine and had begun to lose weight towards the end of the protocol.

Having demonstrated that tumor nodules remained in the peritoneal cavity of mice from all treatment groups, histological analysis was carried out on the major stomach-associated nodules to further examine the tumor microenvironment and location of viral protein. H&E staining of tissue sections (Fig. 6c), utilized to study the structural organization of tumor nodules, demonstrated that the MKN-45-Luc tumors were poorly differentiated. Intracellular EV1 protein was identified in areas distributed throughout the nodules using immunohistochemical analysis in the 1×10^3 TCID₅₀ EV1 groups (Fig. 6c). No obvious differences in EV1 protein distribution existed between the EV1 treatment dose groups (data not shown).

Discussion

Patient prognosis following the peritoneal dissemination of gastric cancer is poor. Surgical resection in combination with regional therapy appears to be the best therapeutic approach. Oncolytic virotherapy is a promising field undergoing extensive investigation, for the targeting and control of cancer. In this study, we demonstrated the efficacy of the naturally occurring oncolytic enterovirus EV1, in gastric cancer cell monolayers and in a novel bioluminescent model of gastric PC.

Oncolytic EV1 targeting of malignant cells requires the cell surface expression of the integrin $\alpha_2\beta_1$, enabling binding of the viral capsid, internalization, and subsequent lytic infection. Integrin $\alpha_2\beta_1$ is involved in the peritoneal

dissemination of gastric cancer cells and tumor cell surface expression is also associated with increased invasiveness and metastases of the liver and lymph nodes [22–26, 37]. The flow cytometric analyses presented in this study demonstrated that each of the gastric cancer cell lines expressed abundant surface levels of the $\alpha_2\beta_1$ integrin. The successful blocking of lytic EV1 infection of MKN-45 cells by the anti- α_2 mAb confirmed the $\alpha_2\beta_1$ receptor-mediated route of entry for oncolytic EV1 infection of gastric cancer cells. In this light, it is plausible that EV1 treatment of PC may not only result in lysis of malignant cells, but may also interfere with the specific interaction between $\alpha_2\beta_1$ and type I collagen, thereby reducing cell adhesion and inhibiting further peritoneal dissemination.

Oncolytic EV1 successfully lysed three of four gastric cancer cell lines at an input multiplicity of less than 1 TCID₅₀/cell, in in vitro monolayer infectivity assays. In particular, MKN-45 and AGS cells were extremely susceptible to oncolysis. Despite the presence of surface $\alpha_2\beta_1$ expression, lysis of the cell monolayer was incomplete in the Hs746T cells, even when infected with a high input multiplicity (>30). A favorable attribute of oncolytic viruses is that they replicate, producing progeny virus capable of circulating to infect neighboring cells and those in metastatic sites, distant to the initial administration site. EV1 underwent efficient replication in the gastric cancer cell lines with a 100- to 1,000-fold amplification of the initial input dose in the susceptible MKN-45, AGS, and NCI-N87 cell lines. The less susceptible Hs746T cells supported EV1 replication, although the maximal yield and rate of replication was less than that observed in the other cell lines and a population of live cells were present 72 h post-infection. EV1 persistently infects the murine 3T3 cell line transfected with human $\alpha_2\beta_1$ yet induces a lytic infection in transfected murine L cells [38]. Persistently infected 3T3 cells displayed comparable levels of $\alpha_2\beta_1$ expression and a delayed rate of viral replication. In the present study, it is possible that a subset of the Hs746T cells were persistently infected, however, further analysis is required to confirm this hypothesis. Another possibility is that the non-infected cells were completely refractile to EV1 lytic infection, possibly as a result of aberrant signalling pathways downstream of the $\alpha_2\beta_1$ integrin, such as those ensuing caveolae-mediated endocytosis of the virus [39].

Cancer cell monolayers are inherently different to the three-dimensional tumor complex. The tumor microenvironment poses both physical and physiological barriers to the successful spread of oncolytic viruses [40]. Analysis of tumor biology and treatment efficacy in mouse models of PC is traditionally difficult to monitor over an extended time period. Gastric PC tumor burden is generally assessed following the sacrifice of mice 1 to 4 weeks post-cell

injection, and analysis carried out via exploratory laparotomy and the weighing and histological examination of involved organs and the peritoneum [10, 12, 13, 26, 41]. Long-term analysis of treatment efficacy is based only on the survival of mice relative to control-treatment groups. Traditionally, the direct measurement of tumor burden over-time has not been feasible. In an attempt to address this situation, cell lines engineered to express fluorescent/luminescent proteins have been developed and utilized in gastric PC models [42, 43], although these have been reliant on fluorostereomicroscopy, which requires prior sacrifice of the mice, and surgical implantation of cells into the gastric wall, respectively. In this study, we described a bioluminescent model of PC reliant on expression of the firefly luciferase gene by MKN-45-Luc cells, for non-invasive real-time imaging, as an effective method for monitoring and measuring peritoneal tumor burden. The well-characterized MKN-45 cells are poorly differentiated gastric cancer cells, originally isolated from a liver metastasis [44] and utilized widely for the gastric PC model [26, 42, 45]. This model required only the intra-peritoneal injection of a cell suspension rather than surgical implantation of cells into the gastric wall, as required in another bioluminescent model [43].

A major finding of this study was that oncolytic EV1 could be successfully utilized for the control of peritoneal dissemination of gastric cancer, in the MKN-45-Luc PC model. The concept of a dose–response relationship following the administration of a replication competent oncolytic virus is difficult to ascertain, as the initial input dose is amplified following infection of the target malignant cells. Previous oncolytic HSV dose-ranging efficacy studies have demonstrated dose–response effects in mouse models of PC [10–12], however the efficacy of doses less than 5×10^5 plaque-forming units have not been reported. In this model, a single intra-peritoneal dose of as little as 1×10^3 TCID₅₀ EV1 was sufficient to significantly reduce peritoneal tumor burden, as indicated by a decrease in tumor cell viability and, by day 28, a positive change in percentage weight from the day of virus administration, indicative of improved health of mice in this group. Although no difference between the doses was evident based on survival analysis or bioluminescence imaging, measurement of weight demonstrated a significant difference between the 1×10^7 and 1×10^3 TCID₅₀ EV1 and between the 1×10^7 TCID₅₀ EV1 and PBS treatment groups, 3 days post-treatment. Importantly, the mice treated with the high EV1 dose displayed weight gain 3 days post-treatment while the groups treated with the medium and low doses initially lost weight following treatment. The difference between the PBS and 1×10^7 TCID₅₀ EV1 groups was still significant 11 days post-treatment, indicating that the initial therapeutic activity of the high EV1 dose

was adequate to improve the health of these mice. A similar result was not observed in mice treated with the medium and low doses of EV1 until 24 days post-treatment, by which time the initial detrimental effects imposed by tumor burden on the digestive tract of the mice were overcome.

Meanwhile, bioluminescence imaging detected a significant difference between each of the EV1 treatment groups and the PBS group 7 days post-treatment, however no significant differences were evident between the virus dose groups. Luminescence is a measure of tumor cell viability, while weight reflects the general health of the animals. The effects of tumor cell death on luminescent output is instantaneous, while an animal requires substantial time to recover from the action of tumors on the digestive tract, resulting in the prolonged differences observed in the weights of the mice. Bioluminescence imaging was not performed until 7 days post-virus administration. Furthermore, picornaviruses display a rapid rate of replication, ranging from 5 to 10 h for a single cycle, depending on the individual virus [32]. In vivo replication of EV1 following intra-peritoneal administration occurred in each of the three treatment dose groups, and the levels of viremia between each of the groups had equalized 7 days post-treatment (approximately 4×10^7 TCID₅₀/mL). At this point, the equivalent levels of viremia displayed by each of the groups would have produced an equivalent effect on tumor cell viability, thus no difference in bioluminescent output was observed in the EV1-treated groups. Following 28 days post-treatment, the level of viremia in all groups decreased by approximately 100-fold and remained stable at this level for the remainder of the observation period (42 days post-treatment). The reduction in the EV1 viremia level occurred at the time point around which mice in each of the groups began to gain weight, suggesting the occurrence of a therapeutic reduction in tumor burden.

Previously, we have shown that a dose of 1×10^5 TCID₅₀ EV1 was adequate for the elimination of subcutaneous and peritoneal ovarian tumors [19]. In a subcutaneous prostate cancer LNCaP model, a dose of 1×10^3 TCID₅₀ EV1 inhibited initial tumor growth while a dose of 1×10^5 TCID₅₀ was required to induce significant tumor regression. Significant anti-cancer activity was observed at an earlier time-point when mice were treated with 1×10^7 TCID₅₀ [18]. The increased efficacy of the 1×10^3 TCID₅₀ EV1 dose in the MKN-45-Luc PC model as compared to the LNCaP model is not surprising as MKN-45 cells display approximately 1,000-fold greater sensitivity than LNCaP cells to in vitro lytic EV1 infection. In addition, we have shown that levels of viremia decline in association with a decrease in ovarian and prostate cancer tumor burden and are undetectable following eradication of tumors [18, 19]. In the MKN-45-Luc PC model, small tumor nodules remained upon sacrifice of the mice,

correlating with continual detection of infectious EV1 in the circulation (approximately 4×10^5 TCID₅₀/mL in each group). Mathematical modelling regimes indicate that a tumor with a slow growth rate, in conjunction with a virus that has a rapid replication rate is more likely to be eradicated, while a tumor with a fast growth rate may outgrow the rate at which the oncolytic virus is able to replicate and lyse cells. Tumor stabilization may result when an equilibrium is established between tumor growth and viral replication rates [46, 47]. The fact that the EV1-treated mice continued to gain weight, tumor bioluminescence continued to decrease and EV1 protein was detected in the major stomach-associated tumors upon sacrifice, in association with the detection of infectious EV1 in the circulation, suggests that it is likely that complete tumor elimination would have eventuated in this model.

In addition to the direct cellular lysis of tumor cells by oncolytic viruses, the role of the immune system in oncolytic virotherapy cannot be underestimated. In particular, virus-specific cytotoxic T lymphocytes (CTL) recruited to recognize viral antigens presented by infected tumor cells and immune-stimulatory signals produced during the viral infection process potentially enhance the therapeutic effect [47]. In contrast, serum neutralizing viral antibodies produced as a result of prior natural exposure or following deliberate administration of the virus may result in premature eradication of the virus, proposing a potential barrier to the systemic administration of oncolytic viruses. Nevertheless, preliminary studies have indicated that the prevalence of neutralizing EV1 antibodies in the population is low, occurring at a rate of approximately 6% [48]. Moreover, a large epidemiological survey of enterovirus serotypes detected in the United States between 1970 and 2005 reported that EV1 represented only 0.4% of identified serotypes [49], indicating that the circulation of EV1 in the community is not widespread.

Surgical resection of abdominal tumors often results in seeding of malignant cells to the peritoneal cavity [50–52]. Trauma induced by laparotomy results in a massive cytokine release and subsequent systemic suppression of the hosts' anti-microbial and anti-tumor immune responses. Minimally invasive laparoscopic surgery, however, results in a suppression of the immune response that is confined to the peritoneum [53, 54]. Hence, a 'therapeutic window' is available following laparoscopy during which EV1, administered intraoperatively, could both directly lyse malignant cells and prevent peritoneal seeding, in the absence of an effective anti-viral response. Having demonstrated the efficacy of EV1 for the treatment of peritoneal dissemination of gastric and ovarian cancer [19], it is conceivable that oncolytic EV1 may also be effective in the therapeutic management of other malignancies that disseminate to the peritoneum, such as colorectal and pancreatic cancers [3, 52].

Other oncolytic viruses, specifically HSVs, adenoviruses and measles virus have displayed therapeutic efficacy following intra-peritoneal delivery in immune-compromised mouse models of peritoneal dissemination, originating from human gastric cancer [11], in addition to ovarian [55–57], pancreatic [58], and renal cancer cell lines [59]. Each of the aforementioned viruses are genetically engineered for attenuation and, or in addition to, enhancement of tumor cell targeting. Unfavorably, engineered viruses may potentially revert to virulent phenotypes or lose their specificity for malignant tissue. In contrast, EV1 is a genetically unmodified, naturally occurring virus of relatively low pathogenicity. The virus was originally isolated from the stools of individuals in the absence of symptomatic infection [30]. EV1 infection is commonly associated with mild upper respiratory infections [32] and, like other enteroviruses, has been implicated in aseptic meningitis [60]. Importantly, the broad-spectrum anti-picornavirus drug, Pleconaril, shortens the duration of illness in severe cases of enteroviral meningitis [61], thus, following therapeutic EV1 administration, infection may be potentially treated in the case of serious side effects. Meanwhile, the tumor cell tropism of EV1 is a result of the elevated surface expression of $\alpha_2\beta_1$ on malignant cells, the natural receptor utilized by the virus for infection. As internalization following $\alpha_2\beta_1$ binding facilitates efficient lytic infection, it is unlikely that genetic selection will pressure EV1 to adapt to a different receptor-mediated route of infection. Finally, pre-existing immunity to some oncolytic viruses may impede therapeutic anti-tumor efficacy. The low incidence of circulating EV1 neutralizing antibodies, as discussed earlier, makes EV1 an attractive candidate for viral therapy. In comparison, the prevalence of neutralizing measles virus antibodies in the population is very high [62], as a result of immunization strategies, while relatively high levels of antibodies resulting from natural exposure to Adenovirus type 5 [63] and HSV-1 [64] exist in the population. Thus, EV1 may demonstrate enhanced efficacy in the targeting and destruction of distant metastases following either intra-peritoneal or intravenous administration.

In summation, we have demonstrated the abundant expression of the $\alpha_2\beta_1$ integrin on the surface of gastric cancer cells. The specific therapeutic targeting of $\alpha_2\beta_1$ by EV1 translated to potent oncolytic activity both in an *in vitro* setting and in an *in vivo* model of peritoneal dissemination of gastric cancer. In addition, we have described a novel bioluminescent model of PC, which enabled real-time non-invasive monitoring of peritoneal tumor burden. Taken together, these results highlight the exciting potential for the application of regional delivery of oncolytic EV1 as a therapeutic for the control of gastric PC.

Acknowledgements We gratefully acknowledge those investigators mentioned in the text for the provision of monoclonal antibodies, vectors, cell lines, and virus that enabled this study to be undertaken. We would also like to thank Dr Erin O'Neill, Jaclyn Stewart, Elise Mac Pherson, Debbie Pepperall, Matthew Bowman, and Brian Krishnan for their valuable technical assistance throughout the project and Dr E. S. Johansson for revision of the manuscript. Funding for this work was provided by Viralytics Ltd.

Funding Darren R. Shafren is a director of Viralytics Pty Ltd. Gough G. Au, Richard D. Barry and Darren R. Shafren hold stock of Viralytics Pty Ltd. and are currently conducting research sponsored by this company.

References

- Parkin DM, Bray F, Ferlay J, Pisani P (2005) Global cancer statistics, 2002. *CA Cancer J Clin* 55:74–108
- Crew KD, Neugut AI (2006) Epidemiology of gastric cancer. *World J Gastroenterol* 12:354–362
- Sadeghi B, Arvieux C, Glehen O, Beaujard AC, Rivoire M, Baulieux J, Fontaumard E, Brachet A, Caillot JL, Faure JL, Porcheron J, Peix JL, Francois Y, Vignal J, Gilly FN (2000) Peritoneal carcinomatosis from non-gynecologic malignancies: results of the EVOCAPE 1 multicentric prospective study. *Cancer* 88:358–363
- Fujiwara Y, Doki Y, Taniguchi H, Sohma I, Takiguchi S, Miyata H, Yamasaki M, Monden M (2007) Genetic detection of free cancer cells in the peritoneal cavity of the patient with gastric cancer: present status and future perspectives. *Gastric Cancer* 10:197–204
- Chu DZ, Lang NP, Thompson C, Osteen PK, Westbrook KC (1989) Peritoneal carcinomatosis in nongynecologic malignancy. A prospective study of prognostic factors. *Cancer* 63:364–367
- Yonemura Y, Endo Y, Obata T, Sasaki T (2007) Recent advances in the treatment of peritoneal dissemination of gastrointestinal cancers by nucleoside antimetabolites. *Cancer Sci* 98:11–18
- Al-Shammaa HA, Li Y, Yonemura Y (2008) Current status and future strategies of cytoreductive surgery plus intraperitoneal hyperthermic chemotherapy for peritoneal carcinomatosis. *World J Gastroenterol* 14:1159–1166
- Bell JC, Garson KA, Lichty BD, Stojdl DF (2002) Oncolytic viruses: programmable tumour hunters. *Curr Gene Ther* 2:243–254
- Parato KA, Senger D, Forsyth PA, Bell JC (2005) Recent progress in the battle between oncolytic viruses and tumours. *Nat Rev Cancer* 5:965–976
- Bennett JJ, Kooby DA, Delman K, McAuliffe P, Halterman MW, Federoff H, Fong Y (2000) Antitumor efficacy of regional oncolytic viral therapy for peritoneally disseminated cancer. *J Mol Med* 78:166–174
- Bennett JJ, Delman KA, Burt BM, Mariotti A, Malhotra S, Zager J, Petrowsky H, Mastorides S, Federoff H, Fong Y (2002) Comparison of safety, delivery, and efficacy of two oncolytic herpes viruses (G207 and NV1020) for peritoneal cancer. *Cancer Gene Ther* 9:935–945
- Stanziale SF, Stiles BM, Bhargava A, Kerns SA, Kalakonda N, Fong Y (2004) Oncolytic herpes simplex virus-1 mutant expressing green fluorescent protein can detect and treat peritoneal cancer. *Hum Gene Ther* 15:609–618
- Kangasniemi L, Kiviluoto T, Kanerva A, Raki M, Ranki T, Sarkioja M, Wu H, Marini F, Hockerstedt K, Isoniemi H, Alftan H, Stenman UH, Curiel DT, Hemminki A (2006) Infectivity-enhanced adenoviruses deliver efficacy in clinical samples and orthotopic models of disseminated gastric cancer. *Clin Cancer Res* 12:3137–3144
- Huang X, Zhuang L, Cao Y, Gao Q, Han Z, Tang D, Xing H, Wang W, Lu Y, Xu G, Wang S, Zhou J, Ma D (2008) Biodistribution and kinetics of the novel selective oncolytic adenovirus M1 after systemic administration. *Mol Cancer Ther* 7:1624–1632
- Shafren DR, Au GG, Nguyen T, Newcombe NG, Haley ES, Beagley L, Johansson ES, Hersey P, Barry RD (2004) Systemic therapy of malignant human melanoma tumors by a common cold-producing enterovirus, Coxsackievirus A21. *Clin Cancer Res* 10:53–60
- Au G, Lincz LF, Enno A, Shafren DR (2007) Oncolytic Coxsackievirus A21 as a novel therapy for multiple myeloma. *Br J Haematol* 137:133–141
- Skelding KA, Barry RD, Shafren DR (2008) Systemic targeting of metastatic human breast tumor xenografts by Coxsackievirus A21. *Breast Cancer Res Treat*. doi:10.1007/s10549-008-9899-2
- Berry LJ, Au GG, Barry RD, Shafren DR (2008) Potent oncolytic activity of human enteroviruses against human prostate cancer. *The Prostate* 68:577–587
- Shafren DR, Sylvester D, Johansson ES, Campbell IG, Barry RD (2005) Oncolysis of human ovarian cancers by echovirus type 1. *Int J Cancer* 115:320–328
- Bergelson JM, St John NF, Kawaguchi S, Pasqualini R, Berdichevsky F, Hemler ME, Finberg RW (1994) The I domain is essential for echovirus 1 interaction with VLA-2. *Cell Adhes Commun* 2:455–464
- Bergelson JM, Shepley MP, Chan BM, Hemler ME, Finberg RW (1992) Identification of the integrin VLA-2 as a receptor for echovirus 1. *Science* 255:1718–1720
- Kawamura T, Endo Y, Yonemura Y, Nojima N, Fujita H, Fujimura T, Obata T, Yamaguchi T, Sasaki T (2001) Significance of integrin alpha2/beta1 in peritoneal dissemination of a human gastric cancer xenograft model. *Int J Oncol* 18:809–815
- Koike N, Todoroki T, Komano H, Shimokama T, Ban S, Ohno T, Fukao K, Watanabe T (1997) Invasive potentials of gastric carcinoma cell lines: role of alpha 2 and alpha 6 integrins in invasion. *J Cancer Res Clin Oncol* 123:310–316
- Nishimura S, Chung YS, Yashiro M, Inoue T, Sowa M (1996) Role of alpha 2 beta 1- and alpha 3 beta 1-integrin in the peritoneal implantation of scirrhous gastric carcinoma. *Br J Cancer* 74:1406–1412
- Matsuoka T, Yashiro M, Nishimura S, Inoue T, Fujihara T, Sawada T, Kato Y, Seki S, Hirakawa-Ys Chung K (2000) Increased expression of alpha2beta1-integrin in the peritoneal dissemination of human gastric carcinoma. *Int J Mol Med* 5:21–25
- Lin MT, Chang CC, Lin BR, Yang HY, Chu CY, Wu MH, Kuo ML (2007) Elevated expression of Cyr61 enhances peritoneal dissemination of gastric cancer cells through integrin alpha2beta1. *J Biol Chem* 282:34594–34604
- Xing L, Huhtala M, Pietiainen V, Vuorinen K, Marjomaki V, Heino J, Johnson MS, Hyypia T, Cheng RH (2004) Structural and functional analysis of integrin alpha2I domain interaction with echovirus 1. *J Biol Chem* 279:11632–11638
- Bergelson JM, Chan BM, Finberg RW, Hemler ME (1993) The integrin VLA-2 binds echovirus 1 and extracellular matrix ligands by different mechanisms. *J Clin Invest* 92:232–239
- Kapyla J, Pentikainen OT, Nyronen T, Nissinen L, Lassander S, Jokinen J, Lahti M, Marjamaki A, Johnson MS, Heino J (2007) Small molecule designed to target metal binding site in the alpha2I domain inhibits integrin function. *J Med Chem* 50:2742–2746
- Melnick JL, Aagren K (1952) Poliomyelitis and coxsackie viruses isolated from normal infants in Egypt. *Proc Soc Exp Biol Med* 81:621–624

31. Couch RB, Cate TR, Gerone PJ, Fleet WF, Lang DJ, Griffith WR, Knight V (1965) Production of illness with a small-particle aerosol of Coxsackie A21. *J Clin Invest* 44:535–542
32. Rancaniello VR (2001) Picornaviridae: the viruses and their replication. In: Fields BN, Knipe DM, Howley PM, Griffin DE, Lamb RA, Martin MA, Roizman B, Straus SE (eds) *Field's virology*. Lippincott Williams and Wilkins, Philadelphia, pp 685–722
33. Dougherty RM (1964) Animal virus titration techniques. In: Harris RJC (ed) *Techniques in experimental virology*. Academic, New York, pp 169–223
34. Yousef GE, Brown IN, Mowbray JF (1987) Derivation and biochemical characterization of an enterovirus group-specific monoclonal antibody. *Intervirology* 28:163–170
35. Samuelson A, Forsgren M, Sallberg M (1995) Characterization of the recognition site and diagnostic potential of an enterovirus group-reactive monoclonal antibody. *Clin Diagn Lab Immunol* 2:385–386
36. Dikmen ZG, Gellert G, Dogan P, Mason R, Antich P, Richer E, Wright WE, shay JW (2005) A new diagnostic system in cancer research: bioluminescent imaging (BLI). *Turk J Med Sci* 35: 65–70
37. Ura H, Denno R, Hirata K, Yamaguchi K, Yasoshima T (1998) Separate functions of alpha2beta1 and alpha3beta1 integrins in the metastatic process of human gastric carcinoma. *Surg Today* 28:1001–1006
38. Zhang S, Racaniello VR (1997) Persistent echovirus infection of mouse cells expressing the viral receptor VLA-2. *Virology* 235:293–301
39. Pietiäinen V, Marjomaki V, Upla P, Pelkmans L, Helenius A, Hyypia T (2004) Echovirus 1 endocytosis into caveosomes requires lipid rafts, dynamin II, and signaling events. *Mol Biol Cell* 15:4911–4925
40. Vaha-Koskela MJ, Heikkilä JE, Hinkkanen AE (2007) Oncolytic viruses in cancer therapy. *Cancer Lett* 254:178–216
41. Yanagihara K, Takigahira M, Tanaka H, Komatsu T, Fukumoto H, Koizumi F, Nishio K, Ochiya T, Ino Y, Hirohashi S (2005) Development and biological analysis of peritoneal metastasis mouse models for human scirrhous stomach cancer. *Cancer Sci* 96:323–332
42. Kaneko K, Yano M, Tsujinaka T, Morita S, Taniguchi M, Fujiwara Y, Doki Y, Inoue M, Shiozaki H, Monden M (2000) Establishment of a visible peritoneal micrometastatic model from a gastric adenocarcinoma cell line by green fluorescent protein. *Int J Oncol* 16:893–898
43. Yanagihara K, Takigahira M, Takeshita F, Komatsu T, Nishio K, Hasegawa F, Ochiya T (2006) A photon counting technique for quantitatively evaluating progression of peritoneal tumor dissemination. *Cancer Res* 66:7532–7539
44. Motoyama T, Hojo H, Watanabe H (1986) Comparison of seven cell lines derived from human gastric carcinomas. *Acta Pathol Jpn* 36:65–83
45. Nakano K, Todo T, Zhao G, Yamaguchi K, Kuroki S, Cohen JB, Glorioso JC, Tanaka M (2005) Enhanced efficacy of conditionally replicating herpes simplex virus (G207) combined with 5-fluorouracil and surgical resection in peritoneal cancer dissemination models. *J Gene Med* 7:638–648
46. Novozhilov AS, Berezovskaya FS, Koonin EV, Karev GP (2006) Mathematical modeling of tumor therapy with oncolytic viruses: regimes with complete tumor elimination within the framework of deterministic models. *Biol Direct* 1:6
47. Wodarz D (2001) Viruses as antitumor weapons: defining conditions for tumor remission. *Cancer Res* 61:3501–3507
48. Karttunen A, Poyry T, Vaarala O, Ilonen J, Hovi T, Roivainen M, Hyypia T (2003) Variation in enterovirus receptor genes. *J Med Virol* 70:99–108
49. Khetsuriani N, Lamonte-Fowlkes A, Oberst S, Pallansch MA (2006) Enterovirus surveillance—United States, 1970–2005. *MMWR Surveill Summ* 55:1–20
50. Yoo CH, Noh SH, Shin DW, Choi SH, Min JS (2000) Recurrence following curative resection for gastric carcinoma. *Br J Surg* 87:236–242
51. Ziprin P, Ridgway PF, Peck DH, Darzi AW (2003) Laparoscopic enhancement of tumour cell binding to the peritoneum is inhibited by anti-intercellular adhesion molecule-1 monoclonal antibody. *Surg Endosc* 17:1812–1817
52. Oosterling SJ, van der Bij GJ, Bogels M, ten Raa S, Post JA, Meijer GA, Beelen RH, van Egmond M (2008) Anti-beta1 integrin antibody reduces surgery-induced adhesion of colon carcinoma cells to traumatized peritoneal surfaces. *Ann Surg* 247:85–94
53. Jung IK, Kim MC, Kim KH, Kwak JY, Jung GJ, Kim HH (2008) Cellular and peritoneal immune response after radical laparoscopy-assisted and open gastrectomy for gastric cancer. *J Surg Oncol* 98:54–59
54. Hegarty N, Dasgupta P (2008) Immunological aspects of minimally invasive oncologic surgery. *Curr Opin Urol* 18:129–133
55. Fu X, Tao L, Zhang X (2007) An oncolytic virus derived from type 2 herpes simplex virus has potent therapeutic effect against metastatic ovarian cancer. *Cancer Gene Ther* 14:480–487
56. Peng KW, TenEyck CJ, Galanis E, Kalli KR, Hartmann LC, Russell SJ (2002) Intraperitoneal therapy of ovarian cancer using an engineered measles virus. *Cancer Res* 62:4656–4662
57. Kanerva A, Zinn KR, Chaudhuri TR, Lam JT, Suzuki K, Uil TG, Hakkarainen T, Bauerschmitz GJ, Wang M, Liu B, Cao Z, Alvarez RD, Curiel DT, Hemminki A (2003) Enhanced therapeutic efficacy for ovarian cancer with a serotype 3 receptor-targeted oncolytic adenovirus. *Mol Ther* 8:449–458
58. Sunamura M, Oonuma M, Motoi F, Abe H, Saitoh Y, Hoshida T, Ottomo S, Horii A, Matsuno S (2002) Gene therapy for pancreatic cancer targeting the genomic alterations of tumor suppressor genes using replication-selective oncolytic adenovirus. *Hum Cell* 15:138–150
59. Guse K, Ranki T, Ala-Opas M, Bono P, Sarkioja M, Rajeci M, Kanerva A, Hakkarainen T, Hemminki A (2007) Treatment of metastatic renal cancer with capsid-modified oncolytic adenoviruses. *Mol Cancer Ther* 6:2728–2736
60. Schleissner LA, Portnoy B (1973) Spectrum of ECHO virus 1 disease in a young diabetic. *CHEST* 63:457–459
61. Desmond RA, Accortt NA, Talley L, Villano SA, Soong SJ, Whitley RJ (2006) Enteroviral meningitis: natural history and outcome of pleconaril therapy. *Antimicrob Agents Chemother* 50:2409–2414
62. McQuillan GM, Kruszon-Moran D, Hyde TB, Forghani B, Bellini W, Dayan GH (2007) Seroprevalence of measles antibody in the US population, 1999–2004. *J Infect Dis* 196:1459–1464
63. Nwanegbo E, Vardas E, Gao W, Whittle H, Sun H, Rowe D, Robbins PD, Gambotto A (2004) Prevalence of neutralizing antibodies to adenoviral serotypes 5 and 35 in the adult populations of The Gambia, South Africa, and the United States. *Clin Diagn Lab Immunol* 11:351–357
64. Xu F, Sternberg MR, Kottiri BJ, McQuillan GM, Lee FK, Nahmias AJ, Berman SM, Markowitz LE (2006) Trends in herpes simplex virus type 1 and type 2 seroprevalence in the United States. *Jama* 296:964–973